Circulation

ORIGINAL RESEARCH ARTICLE

Artery-Associated Sympathetic Innervation Drives Rhythmic Vascular Inflammation of Arteries and Veins

BACKGROUND: The incidence of acute cardiovascular complications is highly time-of-day dependent. However, the mechanisms driving rhythmicity of ischemic vascular events are unknown. Although enhanced numbers of leukocytes have been linked to an increased risk of cardiovascular complications, the role that rhythmic leukocyte adhesion plays in different vascular beds has not been studied.

METHODS: We evaluated leukocyte recruitment in vivo by using real-time multichannel fluorescence intravital microscopy of a tumor necrosis factor-α–induced acute inflammation model in both murine arterial and venous macrovasculature and microvasculature. These approaches were complemented with genetic, surgical, and pharmacological ablation of sympathetic nerves or adrenergic receptors to assess their relevance for rhythmic leukocyte adhesion. In addition, we genetically targeted the key circadian clock gene *Bmal1* (also known as *Arntl*) in a lineage-specific manner to dissect the importance of oscillations in leukocytes and components of the vessel wall in this process.

RESULTS: In vivo quantitative imaging analyses of acute inflammation revealed a 24-hour rhythm in leukocyte recruitment to arteries and veins of the mouse macrovasculature and microvasculature. Unexpectedly, although in arteries leukocyte adhesion was highest in the morning, it peaked at night in veins. This phase shift was governed by a rhythmic microenvironment and a vessel type–specific oscillatory pattern in the expression of promigratory molecules. Differences in cell adhesion molecules and leukocyte adhesion were ablated when disrupting sympathetic nerves, demonstrating their critical role in this process and the importance of β_2-adrenergic receptor signaling. Loss of the core clock gene *Bmal1* in leukocytes, endothelial cells, or arterial mural cells affected the oscillations in a vessel type–specific manner. Rhythmicity in the intravascular reactivity of adherent leukocytes resulted in increased interactions with platelets in the morning in arteries and in veins at night with a higher predisposition to acute thrombosis at different times as a consequence.

CONCLUSIONS: Together, our findings point to an important and previously unrecognized role of artery-associated sympathetic innervation in governing rhythmicity in vascular inflammation in both arteries and veins and its potential implications in the occurrence of time-of-day–dependent vessel type–specific thrombotic events.

Alba de Juan, PhD
et al

Full author list is available on page 1113.

Key Words: cell adhesion molecules ■ circadian rhythm ■ sympathetic nervous system ■ thrombosis

Sources of Funding, see page 1113

https://www.ahajournals.org/journal/circ

Clinical Perspective

What Is New?

- Leukocytes adhere to arteries and veins following a circadian rhythm in mice, with adhesion peaking in arteries in the morning and in veins at night.

What Are the Clinical Implications?

- These peaks in leukocyte adhesion at different times in the 2 vascular beds are associated with increased vascular inflammation and shortened times to local vaso-occlusive events, occurring out of phase between arteries and veins, providing mechanistic insights into the observed time-of-day dependency of cardiovascular complications in patients.

Acute cardiovascular complications in humans occur predominantly at the onset of the behavioral activity phase.[1] Studies have established a correlation between heightened systemic blood leukocyte counts and an increased risk for cardiovascular complications.[2] Specifically, the process of leukocyte recruitment to tissues and the associated intravascular interactions between adherent leukocytes and other free-flowing components of the blood exacerbate vaso-occlusive crises[3,4] and lipopolysaccharide-induced lethality.[5] Recent evidence points to a critical role for circadian leukocyte adhesion in the time-of-day–dependent onset of acute vascular inflammation.[6–10] Although steady-state leukocyte recruitment to tissues occurs almost exclusively from venules, inflammation also induces leukocyte adhesion in arteries.[11] Inflammatory cells, predominantly neutrophils and inflammatory monocytes, roll along and adhere to the vascular endothelium via interactions mediated by E- and P-selectin, chemokines, and the leukocyte integrins leukocyte function–associated antigen-1 (CD11a/CD18) and macrophage-1 antigen (CD11b/CD18) with endothelial intercellular adhesion molecule-1 (ICAM-1) and vascular cell adhesion molecule-1 (VCAM-1).[12–14]

Circadian rhythms exhibit a period length of ≈24 hours and play a critical role in the adaptation of organisms to the rhythmic light-dark changes of the environment.[15–17] Light can entrain these rhythms, leading to the synchronization of rhythms in the suprachiasmatic nuclei of the hypothalamus, which constitute the master clock of the organism. From there, humoral and neural output mechanisms synchronize clocks in peripheral tissues, thus setting a common phase across the body. The sympathetic nervous system regulates the rhythmic and systemic release of glucocorticoids, adrenaline, and noradrenaline from the adrenal glands.[18,19] In addition, sympathetic nerves directly innervate tissues and can modulate physiology locally via the release of noradrenaline from their varicosities.[20] Local versus systemic application of an inflammatory stimulus can cause different outcomes in the ability of neutrophils to reach inflammatory sites,[7,8,21] indicating the importance of confined environmental signals in inflammatory reactions. Whether sympathetic tone can modulate the inflammatory response in a tissue-specific manner has not been defined. Furthermore, the role of sympathetic nerves in inflammation of distinct vascular beds remains unknown. Here, we show that artery-associated sympathetic innervation is critical for oscillatory inflammatory leukocyte adhesion to both arteries and veins with a functional relevance for the temporal incidence of acute thrombotic events.

METHODS

The data that support the findings of this study are available from the corresponding author on reasonable request.

Animals

We used 8- to 10-week-old male mice for all the experiments. *Bmal1*$^{flox/flox}$ (brain and muscle ARNTL-like), *Lyz2cre*, and *Icam1*$^{-/-}$ mice were purchased from Jackson Laboratories. *Ng2-cre* (neuron-glial antigen) and *Ng2-DsRed* (*Cspg4-DsRed*) mice were provided by Konstantin Stark. *Lyz2* (lysozyme)-*gfp* (green fluorescent protein) mice were provided by Markus Sperandio. *Per1*$^{-/-}$*Per2*$^{-/-}$ mice were provided by Urs Albrecht.[22] *Cdh5*^{ERT2}*-cre* mice were a gift from Ralf H. Adams. *Adrb2*$^{-/-}$ (β_2-adrenergic) receptor mice were a gift from Gerard Karsenty to P.S.F. *Nes* (nestin)-*gfp* mice were a gift from Grigori Enikolopov to P.S.F. C57BL/6 wild-type mice were obtained from Charles River. Animals were housed under a 12 hour:12 hour light-dark cycle with ad libitum access to food and water. All animal experimental procedures were carried out in accordance with the German Law of Animal Welfare and approved by the Regierung of Oberbayern or the Animal Care and Use Committee of the Albert Einstein College of Medicine or the Swiss Federal Veterinary Office.

Multichannel Fluorescence Intravital Microscopy

For multichannel fluorescence intravital microscopy of the carotid artery and jugular vein, mice were anesthetized by intraperitoneal injection of ketamine (100 mg/kg), xylazine (20 mg/kg), and acepromazine (1%). A ventral incision was made in the neck, and the carotid artery and jugular vein were exposed. Suture thread was placed around the sternocleidomastoid muscle, and the muscle was pulled to the side. Two surgical knots were placed around the tendon, and a cut was made in the middle to separate the tendon and make the carotid visible. An additional suture thread was then tied around the bone and used to pull it to the side (see also the work by Chèvre et al[23]). Afterward, the exposed area was covered with tumor necrosis factor-α (TNF-α) (150 ng in 100 µL PBS, containing 0.1% BSA) for 2 hours before imaging. In the meantime, a catheter was inserted into the femoral artery for administrating a PE–anti-CD11a antibody (clone M17/4, 1 µg,

Biolegend) in a very low dose to visualize adherent leukocytes. Videos were acquired on a fixed-stage Zeiss Axio Examiner. D1 microscope equipped with a Colibri epifluorescence 405-, 488-, 563-, and 655-nm LED excitation light source (Zeiss).

For multichannel fluorescence intravital microscopy of the cremaster muscle, TNF-α was injected intraperitoneally or into the scrotum 3 hours before imaging. Mice were anesthetized with fentanyl (0,5 mg/kg), midazolam (5 mg/kg), and medetomidine (0,5 mg/kg) via intraperitoneal injection. First, a catheter was inserted in the femoral artery for administration of antibodies in different combinations: PE–anti-Ly6G (clone 1A8, 1 μg, BD Biosciences), DyLight649-GPIbβ (3 μg, Emfret Analytics), PE–anti-CD11b (clone M1/70, 1 μg, Biolegend), and APC–anti-CD62L (clone MEL-14, 1 μg, Biolegend). Preparation of the cremaster muscle was subsequently performed as explained in a previous publication.[7] Specifically, the right testis was exposed through an incision of the scrotum. The cremaster muscle surrounding the testis was opened ventrally in a zone with less vasculature, with electrocautery used to cut the muscle and at the same time to stop any bleeding, and spread over a Plexiglas cube of a custom-made microscopy stage. Epididymis and testicle were detached from the cremaster muscle by electrocautery and placed back into the peritoneum. During the procedure and after surgical preparation, the muscle was superfused with warm saline (0.9% NaCl). Videos were acquired on a fixed-stage Zeiss Axio Examiner.D1 microscope as described above.

Adoptive Transfer Experiments

Single-cell suspensions were obtained from spleen, and bone marrow was obtained from donor mice. Red blood cells were lysed, and the remaining cells were resuspended in cell incubation buffer (PBS, 0.2% BSA, 2 mmol/L EDTA). Bone marrow and spleen cells were mixed at a ratio of 50:50 and labeled with 1.5 μmol/L carboxyfluorescein succinimidyl ester (ThermoFisher Scientific) for 20 minutes at 37°C. Afterward, cells were washed 3 times and resuspended in PBS. Labeled cells (20×10^6) were injected intravenously into each recipient mouse. Simultaneously, TNF-α was applied topically on the exposed carotid artery and the jugular vein. After 2 hours, artery and vein were harvested from recipient mice and digested to obtain single-cell suspensions for flow cytometry with collagenase IV (Sigma; 1 mg/mL), DNase I (Roche; 0.2 mg/mL), and collagenase D (Roche-Sigma; 3.5 mg/mL) for 30 minutes at 37°C and smashed through 70-μm cell strainers (ThermoFisher Scientific). Single-cell suspensions were stained with antibodies purchased from Biolegend (1:200 dilution) against PE–anti-CD11a (clone M17/4), PE/DZL594–anti-CD45 (clone 30-F11), PerCP/Cy5.5–anti-Gr-1 (clone RB6-8C5), PE/Cy7-gp38 (clone 8.1.1.), APC–anti–platelet endothelial cell adhesion molecule-1 (clone MEC13.3), and Brilliant Violet 510–anti-F4/80 (clone BM8). DAPI (Biolegend) was used to identify dead cells.

Functional Blocking of Adhesion Molecules and Chemokine Receptors

Animals were injected intravenously with 200 μg of the following blocking antibodies (BioxCell): anti-CD54 (ICAM-1; clone YN1/1.7.4), anti-CD106 (VCAM-1; clone M/K-2.7), or their isotypes (for ICAM-1 clone LTF-2 and for VCAM-1 clone HRPN) or antagonists against the chemokine receptors CXCR2 and CCR2 (5 mg/kg, Tocris) 1 hour before stimulation with TNF-α and 3 hours before in vivo imaging experiments. In the case of the chemokine antagonist, 1% Tween80 and 5% dimethyl sulfoxide in PBS were used as vehicle controls.

Denervation Techniques

Mice were denervated in 2 different ways: chemically with 6-hydroxydopamine and surgically via removal of the superior cervical ganglion. For the chemical denervation, 6-hydroxydopamine was dissolved in ascorbic acid solution at 20 mg/mL (in PBS) and injected twice before the experiment. A first dose of 100 mg/kg was followed by a second dose of 250 mg/kg 2 days later, and in vivo imaging was performed 3 days later. For the surgical denervation, a ventral incision was made in the neck, and the superior cervical ganglion, located underneath the carotid bifurcation, was removed unilaterally by careful dissection with forceps. On the contralateral side, a sham procedure was carried out without cutting the ganglion. The incision on the neck was closed, and the mice were left to recover for 4 weeks to re-establish normal blood leukocyte levels indicating the absence of inflammation.

β_2-Adrenergic Receptor Antagonist/Agonist Treatment

For the purpose of investigating β_2-adrenergic receptor function, the antagonist butoxamine or the agonist clenbuterol (Sigma-Aldrich) was administered via intraperitoneal injection (5 mg/kg). For short-term treatments, injections were performed 2 hours before imaging. For long-term treatments, injections were performed for 5 consecutive days, and imaging was performed 24 hours after the last injection.

Thrombosis Assay

Mice were anesthetized with fentanyl (0.5 mg/kg), midazolam (5 mg/kg), and medetomidine (0.5 mg/kg) via intraperitoneal injection, and a catheter was inserted into the femoral artery for the administration of FITC-coupled dextran (2.5% 500 kDa). Once the catheter was placed in the artery, the surgical preparation of the cremaster muscle was performed as explained before. An initial amount of 100 μL FITC-coupled dextran was given to the mice through the catheter, and fluorescence was measured until it reached 1800 arbitrary units inside the vessel. Fluorescence levels were kept constant by obtaining digital images from each vessel and checking the mean fluorescence intensity. FITC phototoxicity was induced with a 488-nm epifluorescence excitation source. This leads to local energy absorption by the dye within the vessel and to endothelial cell damage with the formation of a thrombus as a consequence. Occlusion time was quantified for multiple vessels in each mouse (3 venules and 3 arterioles of the same size, 60- and 40-μm diameter, respectively).

Statistics

Statistical analyses were performed with GraphPad Prism 6 software. All data are represented as mean±SEM. To compare 2 groups, an unpaired Student *t* test was performed. In case

of unequal variances, the *t* test was combined with the Welch correction. For nonparametric analyses, a Mann–Whitney test was performed. For ≥3 groups, 1-way ANOVA followed by the Tukey post hoc test or 2-way ANOVA followed by the Bonferroni post hoc test was used. Statistical significance was assessed as **P*<0.05, ***P*<0.01, ****P*<0.001, and *****P*<0.0001.

RESULTS

Inflammatory Leukocyte Adhesion to Arteries and Veins Occurs at Different Times of the Day

We set out to perform a detailed investigation into time-of-day–dependent leukocyte recruitment patterns to arteries and veins in an acute inflammatory scenario. Mice were treated locally with TNF-α, and interactions between leukocytes and the vessel wall were visualized in real time in the carotid artery and the jugular vein of the same animals by multichannel fluorescence intravital microscopy and low-dose injections of fluorescent antibodies. Interestingly, leukocyte adhesion in the artery exhibited a striking diurnal rhythmicity (Figure 1A). Moreover, we observed a strong oscillation in leukocyte adhesion in veins, but this rhythm exhibited an unexpected phase shift compared with arteries (Figure 1B and 1C). In the artery, adhesion peaked in the early morning (Zeitgeber time [ZT] 1, ie, 1 hour after light onset in a 12 hour:12 hour light:dark environment) and troughed around midnight (ZT17). In contrast, leukocyte adhesion in the vein reached a trough in the morning and peaked at midnight. Local hemodynamic parameters showed no apparent change between day and night conditions in either vascular bed (data not shown). We confirmed these observations in *Lyz2-gfp* mice, in which myeloid cells are fluorescently labeled genetically (Figure 1D). We next investigated whether this phenomenon was specific for the macrovasculature and the investigated heterogeneous set of large-caliber vessels situated anatomically apart or whether the same held true for an organ-embedded microvascular bed in which arteries and veins share close proximity. Using multichannel fluorescence intravital microscopy of the cremaster muscle microcirculation, we detected a similar time-dependent leukocyte adhesion pattern in smaller arterioles and venules (Figure 1E). In addition, changes in rolling velocities were observed in both vessels (Figure IA in the online-only Data Supplement), peaking at night in arterioles and in venules in the morning, a sign of lower levels of tissue activation[24] (Figure IA in the online-only Data Supplement). This indicated that these rhythms occur in both small- and large-caliber vessels. These data provide for the first time evidence that inflammatory leukocyte recruitment to arteries and veins is diurnally regulated with distinct rhythmicity depending on the type of vascular bed.

Arterial and venous blood exhibited similar daily changes in leukocyte counts, excluding the possibility that adhesion in arteries might downmodulate venous adhesion levels downstream of the vascular tree simply by reducing the numbers of available circulating cells (Figure IB in the online-only Data Supplement). We next investigated whether the distinct rhythms in both vascular beds were governed by the leukocyte or the microenvironment. We first focused on whether the circadian clock in leukocytes could drive rhythmicity, targeting the key circadian gene *Bmal1*. Interestingly, *Lyz2cre:Bmal1*$^{flox/flox}$ mice, which exhibit a *Bmal1* deficiency specifically in myeloid cells, no longer displayed oscillations in recruitment to arteries or veins (Figure 2A and 2B). This implied that the circadian clock in myeloid cells plays a critical role in rhythmic leukocyte adhesion, likely via a common mechanism in both vascular beds. However, that loss of *Bmal1* in myeloid cells affected rhythmicity in both arteries and veins did not explain the observed phase shift between the vessel types and suggested that the vessels mediated the altered adhesion rhythms between arteries and veins.

We thus focused in subsequent assays on the influence of the microenvironment. We performed adoptive transfer assays using fluorescently labeled leukocytes harvested from donors during the day, injected them simultaneously into 12 hour:12 hour light:dark–entrained recipients during their respective day or night phase, and performed flow cytometry of the harvested carotid arteries and jugular veins. In this setting, a functional importance of rhythmicity only in the microenvironment was assessed. Transferred leukocytes were recruited with different rhythmicity to arteries and veins (Figure 2C), and neutrophils were the main cell type (Figure 2D and Figure IC in the online-only Data Supplement). These results were in line with our in vivo adhesion data and suggested that different oscillations in the microenvironment were responsible for the observed phase shift in leukocyte adhesion. We thus next assessed the role of the circadian clock in endothelial cells, situated at the blood-tissue interface and acting as critical regulators of leukocyte adhesion,[12–14] in mediating rhythmicity and a phase shift between the 2 vascular beds. Interestingly, *Cdh5cre*^{ERT2}*:Bmal1*$^{flox/flox}$ mice, which lack *Bmal1* expression selectively in endothelial cells, exhibited no more oscillations in venous leukocyte adhesion but still showed rhythmicity in arterial adhesion (Figure 2E and 2F). The latter was confirmed in mice deficient in *Bmal1* only in arterial endothelial cells (*Bmxcre*^{ERT2}*:Bmal1*$^{flox/flox}$; Figure ID in the online-only Data Supplement). This implied a role for the circadian clock in venous, but not arterial, endothelial cells in the process and provided a potential explanation for the phase shift in adhesion between both tissues. Furthermore, the results demonstrated that both the leukocyte

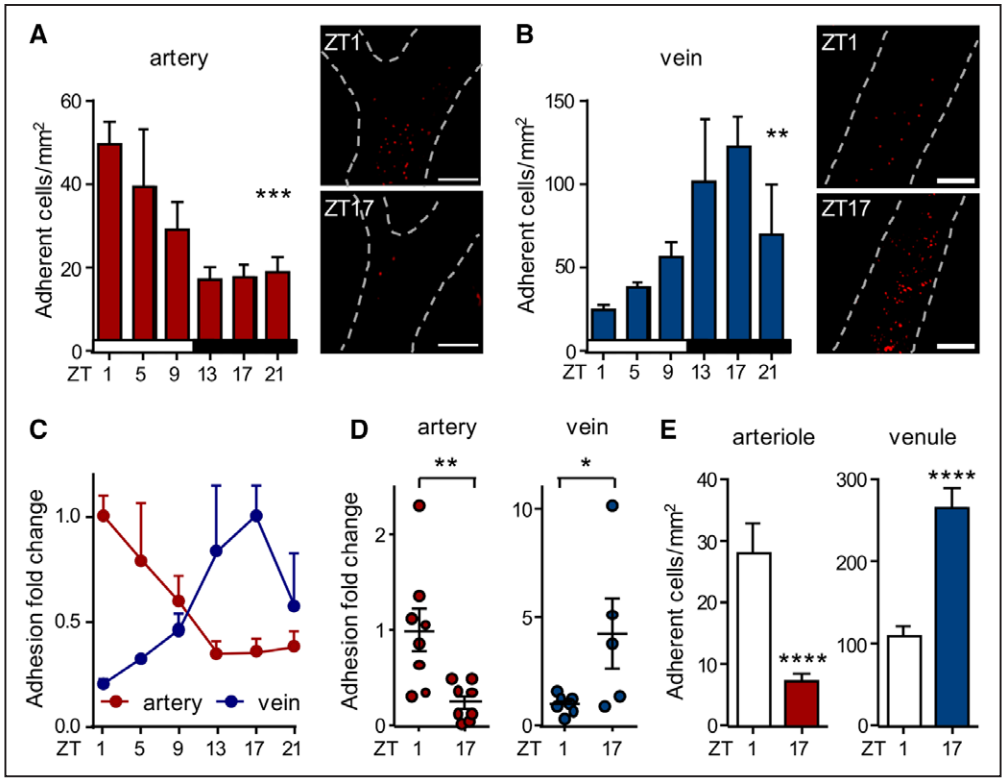

Figure 1. Inflammatory leukocyte adhesion to arteries and veins occurs at different times of the day.
A and **B**, In vivo quantification of adherent leukocytes after tumor necrosis factor-α (TNF-α) stimulation over 24 hours in carotid artery (**A**) and jugular vein (**B**); n=4 to 13 mice, 1-way ANOVA. **C**, Normalization of the leukocyte adhesion data from **A** and **B**. Data are normalized to peak levels; n=4 to 13 mice. **D**, In vivo quantification of adherent cells in *Lyz2-gfp* mice after TNF-α stimulation in carotid artery and jugular vein. Data are normalized to Zeitgeber time (ZT) 1-hour levels; n=5 to 8 mice, Student *t* test (artery) and Mann–Whitney test (vein). **E**, In vivo quantification of adherent cells in arterioles and venules of the cremasteric microvasculature after TNF-α stimulation; n=5 mice, Student *t* test. Scale bars, 200 μm. **P*<0.05; ***P*<0.01; ****P*<0.001; *****P*<0.0001.

and the microenvironment are involved in the diurnal adhesion rhythms.

Altered Rhythmicity in Promigratory Molecules in Arteries and Veins

We next focused on the potential molecules mediating leukocyte adhesion. Quantitative polymerase chain reaction analyses of carotid arteries and jugular veins for promigratory factors showed oscillatory mRNA expression profiles for *Icam1* in both arteries and veins, whereas *Vcam1*, E-selectin (*Sele*), and P-selectin (*Selp*) were oscillatory only in venous tissue (Figure 3A). In addition, we observed temporal differences in both tissues for *Cxcl1, Cxcl2*, and *Ccl2*, critical chemokines for myeloid cell trafficking[25] (Figure 3B). In line with the in vivo recruitment data, expression levels for these molecules peaked in the morning in arteries but at night in the veins, indicating their potential involvement in this process (Figure 3A and 3B). We quantified protein expression levels of cell adhesion molecules specifically in endothelial cells using frozen tissue sections of carotid arteries and jugular veins. ICAM-1 and VCAM-1 levels peaked at day onset for the artery and at night for the vein (Figure 3C and 3D). We also observed oscillations in E-selectin in veins but not arteries, whereas P-selectin was not rhythmically expressed (Figure 3C and 3D and data not shown). We therefore focused on the adhesion-mediating molecules ICAM-1 and VCAM-1 in subsequent functional assays. Mice treated with anti–ICAM-1– or anti–VCAM-1–blocking antibodies and *Icam1*-deficient mice exhibited no more temporal differences in leukocyte adhesion to both arteries and veins (Figure 3E and 3F). Furthermore, blocking their integrin ligands on leukocytes (leukocyte function–associated antigen-1 and macrophage-1) ablated oscillations in a similar manner (Figure 3E). Inhibiting CCR2 function also reduced levels of adhesion and ablated time-of-day differences in both vessels, whereas blocking CXCR2 affected rhythmicity only in veins, confirming the functional importance of these chemokine receptors in mediating adhesion rhythmicity (Figure 3G). Although arterial adhesion relied heavily on ICAM-1, VCAM-1, macrophage-1, and CCR2 for rhythmic adhesion, in veins, leukocyte function–associated antigen-1 and CXCR2 played additional roles. These results indicated that distinct microenvironmental rhythms in the expression of promigratory factors in arteries and veins were the critical determinants for the inverted leukocyte adhesion patterns.

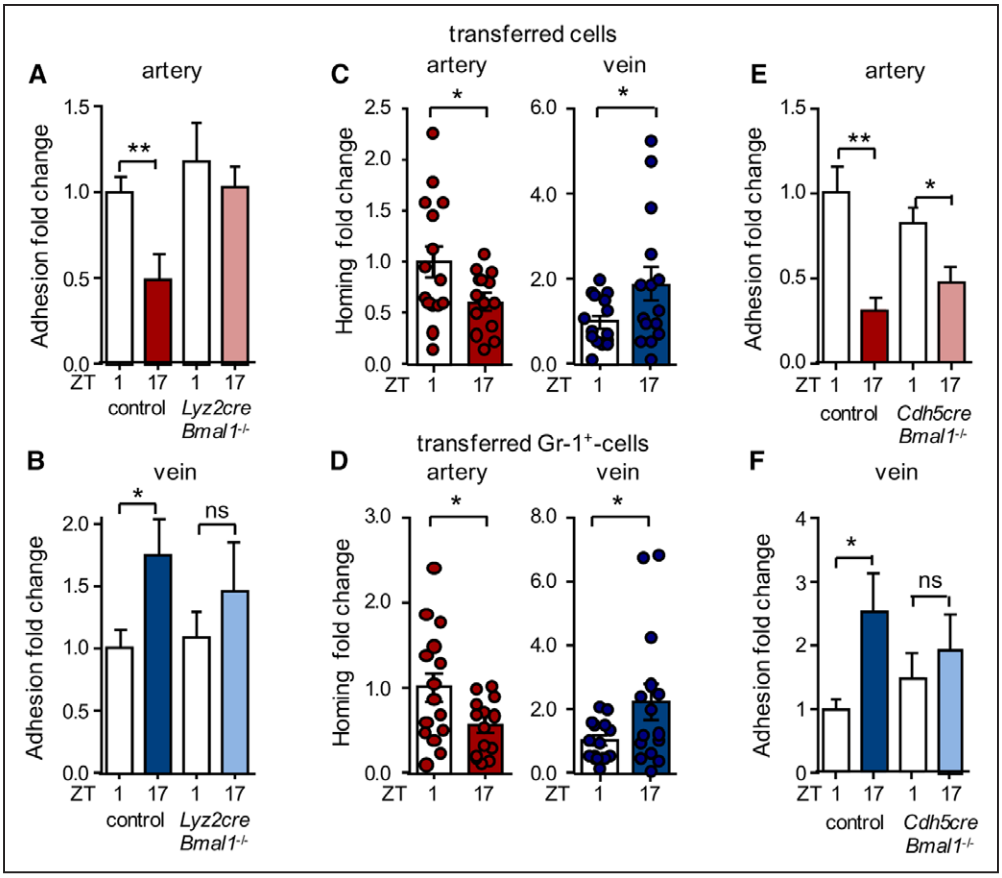

Figure 2. Role of rhythmicity in myeloid cells and the microenvironment.
A and **B**, In vivo quantification of adherent leukocytes after tumor necrosis factor-α (TNF-α) stimulation in carotid artery (**A**) and jugular vein **(B)** in control and *Lyz2cre:Bmal1*$^{-/-}$ mice. Data are normalized to control Zeitgeber time (ZT) 1-hour levels; n=7 to 10 mice, Student *t* test. **C**, Homing experiments of adoptively transferred leukocytes (**C**) and Gr1^{+} cells (**D**) to carotid artery and jugular vein after TNF-α stimulation. Data are normalized to ZT1 levels; n=13 to 15 mice, Student *t* test with Welch correction. **E** and **F**, In vivo quantification of adherent leukocytes after TNF-α stimulation in carotid artery (**E**) and jugular vein (**F**) in control and *Cdh5cre*^{ERT2}*:Bmal1*$^{-/-}$ mice. Data are normalized to control ZT1 levels; n=8 to 11 mice, Student *t* test with Welch correction. ns indicates nonsignificant. **P*<0.05; ***P*<0.01.

Similar Circadian Clock Phases in Arteries and Veins

We therefore next examined whether overall circadian rhythmicity was altered between arteries and veins using *Per2:luc* mice, in which luciferase expression is driven by the rhythmically expressed clock gene *Per2*.[26] Harvested arteries and veins exhibited marked circadian oscillations in luciferase expression over multiple days in culture, with arteries showing a much more pronounced rhythm than veins and exhibiting peaks at slightly different phases (Figure 4A). Previous data have indicated different circadian phases in arteries and veins,[27] but these slight changes in peak times likely do not explain the dramatic phase shifts observed in leukocyte adhesion. In addition, quantitative polymerase chain reaction analyses of the core circadian clock genes *Bmal1*, *Clock, Per1, Per2, Cry1, Nr1d1, Nr1d2, Rora*, and *Rorc* and the output gene D-site of albumin promoter (*Dbp*) under both steady-state and inflamed conditions revealed peaks and troughs in arteries and veins occurring at very similar times in the light cycle (Figure 4B through 4D). These data indicated that clock genes are expressed in a phase between arteries and veins, making it unlikely that a phase shift in the overall oscillations of these tissues was responsible for the distinct leukocyte adhesion patterns.

Local Sympathetic Innervation Drives Rhythmic Inflammatory Responses

Because oscillations of core clock genes in arteries and veins occurred at similar times, we speculated that our observations resulted from a difference in the inflammatory response to TNF-α stimulation. However, *Tnfrsf1a* and *Tnfrsf1b* expression (as well as that of *Nr3c1,* encoding the glucocorticoid receptor) was nonrhythmic in both arteries and veins (Figure IIA through IID in the online-only Data Supplement), making it unlikely that a simple difference in TNF-α sensing was responsible. We therefore investigated a potential involvement of upstream factors in this process, focusing on sympathetic input as a potential mechanism.[28] We performed a systemic chemical sympathectomy of mice by administer-

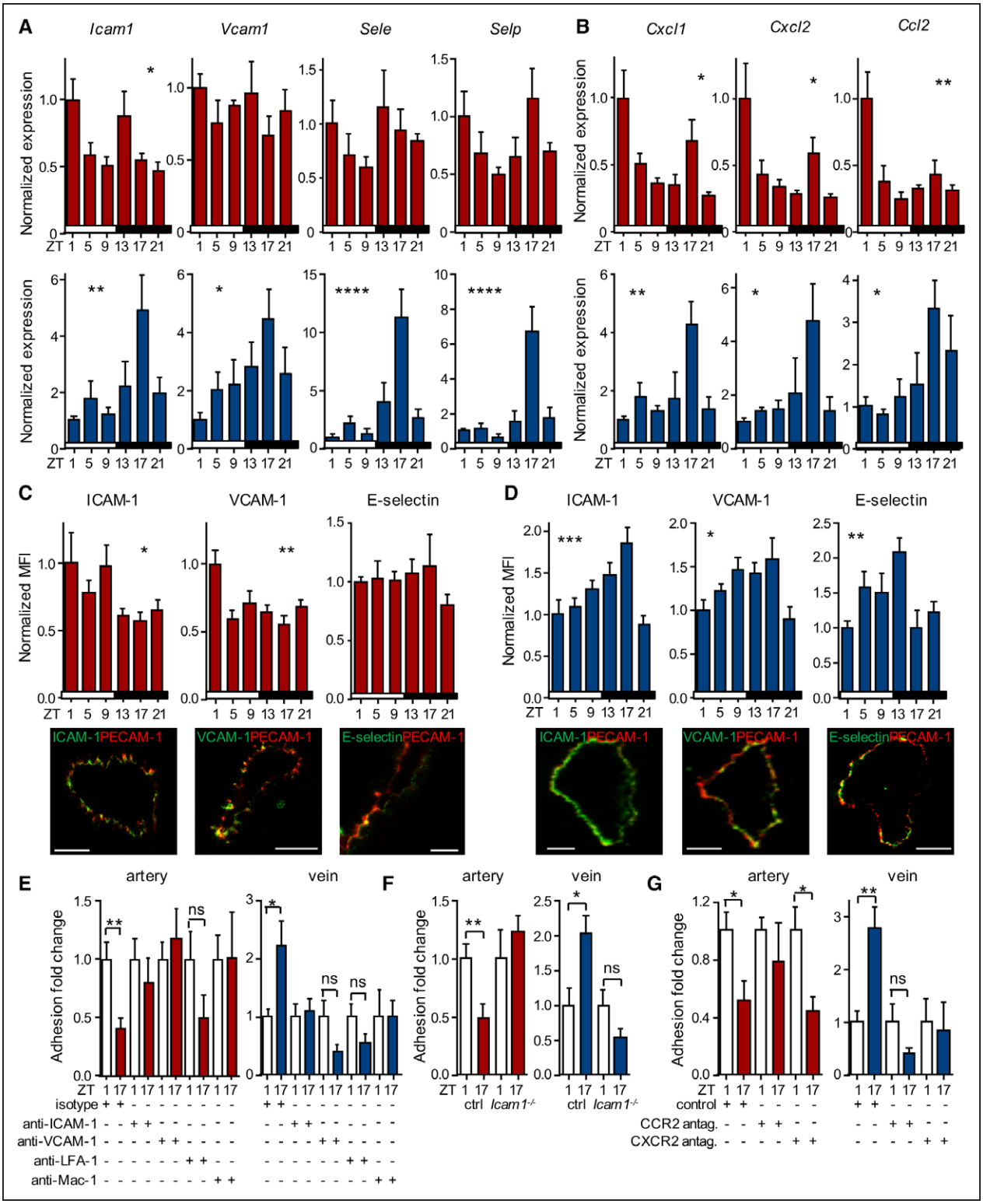

Figure 3. Distinct rhythmicity of promigratory molecules in arteries and veins.
A and **B**, Quantitative polymerase chain reaction analyses of cell adhesion molecules (**A**) and chemokines (**B**) in carotid artery (red) and jugular vein (blue) after tumor necrosis factor-α (TNF-α) stimulation over the course of the day; n=3 to 6 mice, 1-way ANOVA. (**C** and **D**) Mean fluorescence intensity (MFI) quantifications and representative images of adhesion molecule expression in endothelial cells after TNF-α stimulation in carotid artery (**C**) and jugular vein (**D**). Data are normalized to Zeitgeber time (ZT) 1-hour levels; n=3 to 6 mice, 1-way ANOVA. **E**, In vivo quantification of adherent leukocytes after TNF-α stimulation in carotid artery and jugular vein after antibody blockade. Data are normalized to ZT1 levels; n=4 to 6 mice, Student *t* test. **F**, In vivo quantification of adherent leukocytes after TNF-α stimulation in carotid artery and jugular vein in *Icam1*$^{-/-}$ mice; n=8 to 9 mice, Student *t* test. **G**, In vivo quantification of adherent leukocytes after TNF-α stimulation in carotid artery and jugular vein after antagonist treatment. Data are normalized to ZT1 levels; n=4 to 6 mice, Student *t* test. Scale bars, 50 μm. ICAM-1 indicates intercellular adhesion molecule-1; LFA-1, lymphocyte function-associated antigen 1; Mac-1, macrophage-1; PECAM-1, platelet endothelial cell adhesion molecule-1; and VCAM-1, vascular cell adhesion molecule-1. *P<0.05; **P<0.01; ***P<0.001; ****P<0.0001.

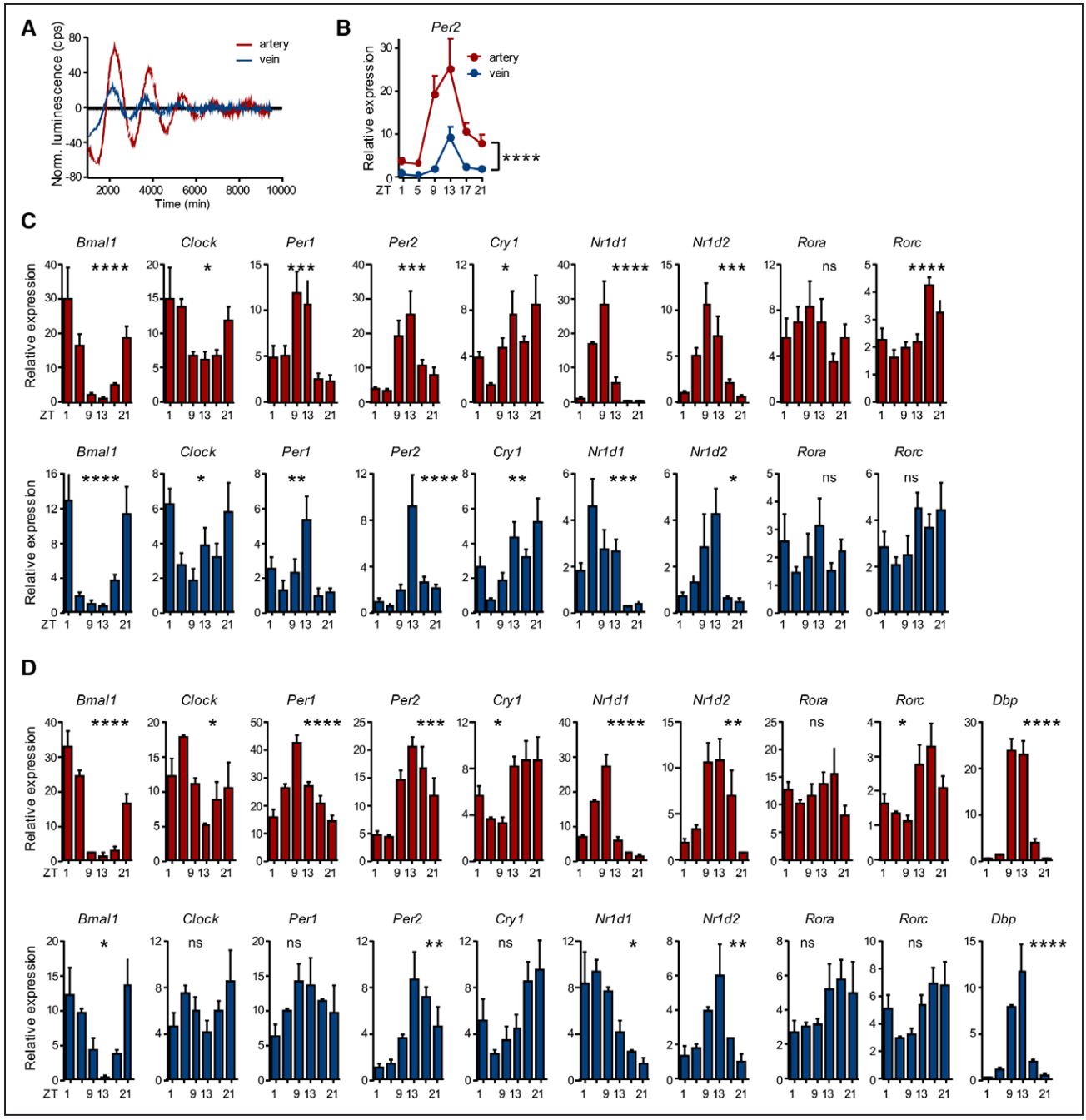

Figure 4. Clock gene expression patterns in arteries and veins.
A, Ex vivo circadian oscillations of *Per2* expression levels as quantified in aorta and vena cava harvested from the bioluminescence *mPer2:Luc* reporter mouse over 6 days under noninflammatory conditions; n=3 mice. **B**, Comparison of *Per2* expression levels between carotid artery (red) and jugular vein (blue) over the course of the day in steady state; n=6 mice, 2-way ANOVA. **C** and **D**, Quantitative polymerase chain reaction analyses of circadian clock gene expression levels over 24 hours in carotid artery (red) and jugular vein (blue) under (**C**) steady-state and (**D**) tumor necrosis factor-α–induced inflammatory conditions; n=6 mice, 1-way ANOVA. **P*<0.05; ***P*<0.01; ****P*<0.001; *****P*<0.0001.

ing 6-hydroxydopamine, a sympathetic neurotoxin. This treatment ablated the temporal differences in leukocyte recruitment to both arteries and veins (Figure 5A), indicating that the sympathetic nervous system played a critical role in mediating oscillatory leukocyte adhesion to both vascular beds. To distinguish between the effects of direct neural input via local sympathetic nerves and humoral circulating factors, we performed microsurgeries to locally ablate the superior cervical ganglion, which is responsible for the direct sympathetic innervation of the head and neck area.[29] Performing these experiments unilaterally while carrying out a sham surgery on the contralateral side allowed us to investigate nerve-intact and denervated vessels in the same mice. We confirmed that the surgery ablated sympathetic input to the ipsilateral side while leaving the contralateral

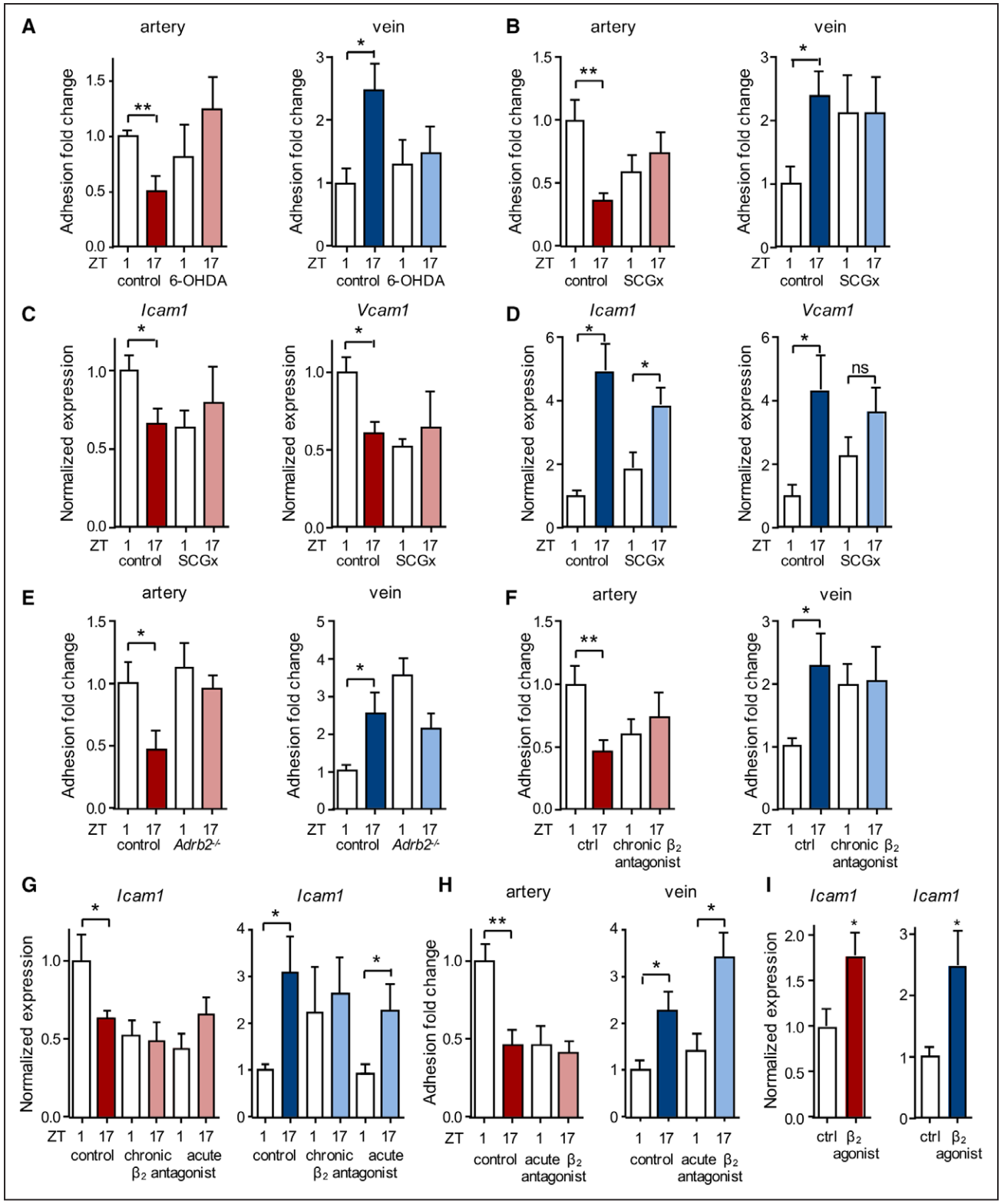

Figure 5. Local sympathetic nerves drive rhythmic inflammatory responses.
A, In vivo quantification of adherent leukocytes after tumor necrosis factor-α (TNF-α) stimulation in carotid artery and jugular vein after 6-hydroxydopamine (6-OHDA) treatment. Data are normalized to Zeitgeber time (ZT) 1-hour control levels; n=5 to 8 mice, Student *t* test. **B**, In vivo quantification of adherent leukocytes after TNF-α stimulation in carotid artery and jugular vein after unilateral surgical denervation of the superior cervical ganglion (SCGx). Data are normalized to ZT1 control levels; n=5 to 12 mice, Student *t* test. **C** and **D**, Quantitative polymerase chain reaction (qPCR) analyses of cell adhesion molecules after TNF-α stimulation in carotid artery (**C**) and jugular vein (**D**) of SCGx mice. Data are normalized to ZT1 control levels; n=4 to 7 mice, Student *t* test with Welch correction. **E**, In vivo quantification of adherent leukocytes after TNF-α stimulation in carotid artery and jugular vein of *Adrb2*$^{-/-}$ mice. Data are normalized to ZT1 control levels; n=6 to 9 mice, Student *t* test. **F**, In vivo quantification of adherent leukocytes after TNF-α stimulation in carotid artery and jugular vein after 5 days (long-term) treatment with a β_2-adrenergic receptor antagonist. Data are normalized to ZT1 control levels; n=4 to 7 mice, Student *t* test with Welch correction. **G**, qPCR (*Continued*)

side intact (Figure IIIA in the online-only Data Supplement). In addition, no effects on vessel diameters were observed (Figure IIIB in the online-only Data Supplement). The superior cervical ganglion ablated temporal differences in leukocyte recruitment in both arteries and veins, whereas in the contralateral sides, rhythms remained intact (Figure 5B). The surgery additionally ablated diurnal oscillations in the expression of promigratory factors in arteries and dampened them in veins (Figure 5C and 5D). This was not caused by ablation of circadian rhythms per se in these tissues because denervated vessels retained rhythmic clock gene expression (Figure IIIC and IIID in the online-only Data Supplement). Thus, sympathetic innervation is not responsible for the rhythmic entrainment of these vascular tissues, consistent with a previous study.[30] Instead, our data imply a critical role for local sympathetic nerves in governing leukocyte adhesion through the rhythmic expression of adhesion molecules to both arteries and veins after an inflammatory insult.

We therefore investigated which adrenoceptors were involved in this process. Expression analyses revealed the presence of *Adrb2* in both arteries and veins and the expression of downstream G-protein–coupled receptor kinases (Figure IVA through IVD in the online-only Data Supplement). No significant oscillation in leukocyte adhesion was observed in both types of vessels of *Adrb2*$^{-/-}$ animals (Figure 5E). To verify that this was not the result of a developmental phenotype, we treated wild-type mice pharmacologically for 5 days using a β_2-adrenergic receptor antagonist. Consistent with the genetic experiments, animals receiving the antagonist exhibited no oscillation in leukocyte recruitment (Figure 5F) or in the expression of promigratory molecules (Figure 5G) without affecting *Bmal1* expression (Figure IVE in the online-only Data Supplement). We next performed the same treatment for a shorter time frame (2 hours) to tease apart potential differences between arteries and veins that might explain their distinct rhythmic inflammatory responses. Interestingly, with this shorter treatment, the functional importance of the β_2-adrenergic receptor was confirmed in the artery, whereas it had no effect in veins (Figure 5G and 5H). In contrast, exogenous, short-term (2 hours) application of a β_2-adrenergic receptor agonist showed an increase in the expression of adhesion molecules in both arteries and veins (Figure 5I). This indicated that both types of vessels could in principle react in a similar manner to β_2-adrenergic stimulation if applied exogenously and thus that differences in local endogenous sympathetic tone and sensitivity were likely responsible for the distinct effects observed in both vessels.

Sympathetic Nerves Are Associated With Arteries

How might sympathetic nerves be able to modulate inflammatory leukocyte recruitment to arteries in a different manner than to veins? To explore this, we performed immunofluorescence imaging analyses of the sympathetic innervation status of arteries and veins in the macrovasculature and microvasculature. Interestingly, although large sympathetic nerve bundles accompanied the carotid artery and cremasteric arterioles exhibited heavy sympathetic innervation, the jugular vein and cremasteric venules were devoid of sympathetic fibers (Figure 6A and 6B). Confirming these results, mRNA expression of tyrosine hydroxylase, the rate-limiting enzyme for the generation of catecholamines in sympathetic nerves, was high in arteries but absent from veins (Figure 6C). Sympathetic nerves innervate arteries at the level of α-smooth muscle actin–positive mural cells[31] (Figure 6D through 6F). These cells coexpress NG2 (Figure 6F through 6H), a marker that is absent from veins that can be used to differentiate between arteries and veins[32–34] (Figure 6G and 6H). We therefore used *Ng2-cre* mice to ablate the circadian gene *Bmal1* in arterial mural cells. Interestingly, *Bmal1* deficiency in NG2$^+$ cells alone resulted in loss of time-of-day differences in *Bmal1* expression in the whole arterial tissue, indicating a critical pacemaker function for these cells in arteries (Figure VA in the online-only Data Supplement). In addition, it ablated the temporal differences in leukocyte adhesion and *Icam1* expression in these tissues (Figure 6I and 6J), a phenotype we also observed in clock-deficient *Per1*$^{-/-}$*Per2*$^{-/-}$ double-knockout mice (Figure VB in the online-only Data Supplement), without affecting systemic blood leukocyte oscillations (Figure VC in the online-only Data Supplement). Although arteries were targeted with this genetic approach, oscillations also ceased in veins (Figure 6I and 6J and Figure VA in the online-only Data Supplement). These data, together with the microsurgical denervation experiments (Figure 5C and 5D), thus indicate that local sympathetic nerves innervating arteries are critical for the oscillatory inflammation process in both arteries and veins. They furthermore demonstrate the critical importance of circadian oscillations in arterial NG2$^+$ mural cells for a rhythmic inflammatory process in both types of vessel.

Figure 5 Continued. analyses of cell adhesion molecules after TNF-α stimulation in carotid artery and jugular vein after long-term (5 days) or short-term (2 hours) treatment with a β_2-adrenergic receptor antagonist. Data are normalized to ZT1 control levels; n=5 to 6 mice, Student *t* test with Welch correction. **H**, In vivo quantification of adherent leukocytes after TNF-α stimulation in carotid artery and jugular vein after 2 hours (short-term) treatment with a β_2-adrenergic receptor antagonist. Data are normalized to ZT1 control levels; n=6 to 11 mice, Student *t* test. **I**, qPCR analyses of cell adhesion molecules after TNF-α stimulation in carotid artery and jugular vein after short-term (2 hours) treatment with a β_2-adrenergic receptor agonist; n=5 to 6 mice, Student *t* test with Welch correction. **P*<0.05; ***P*<0.01.

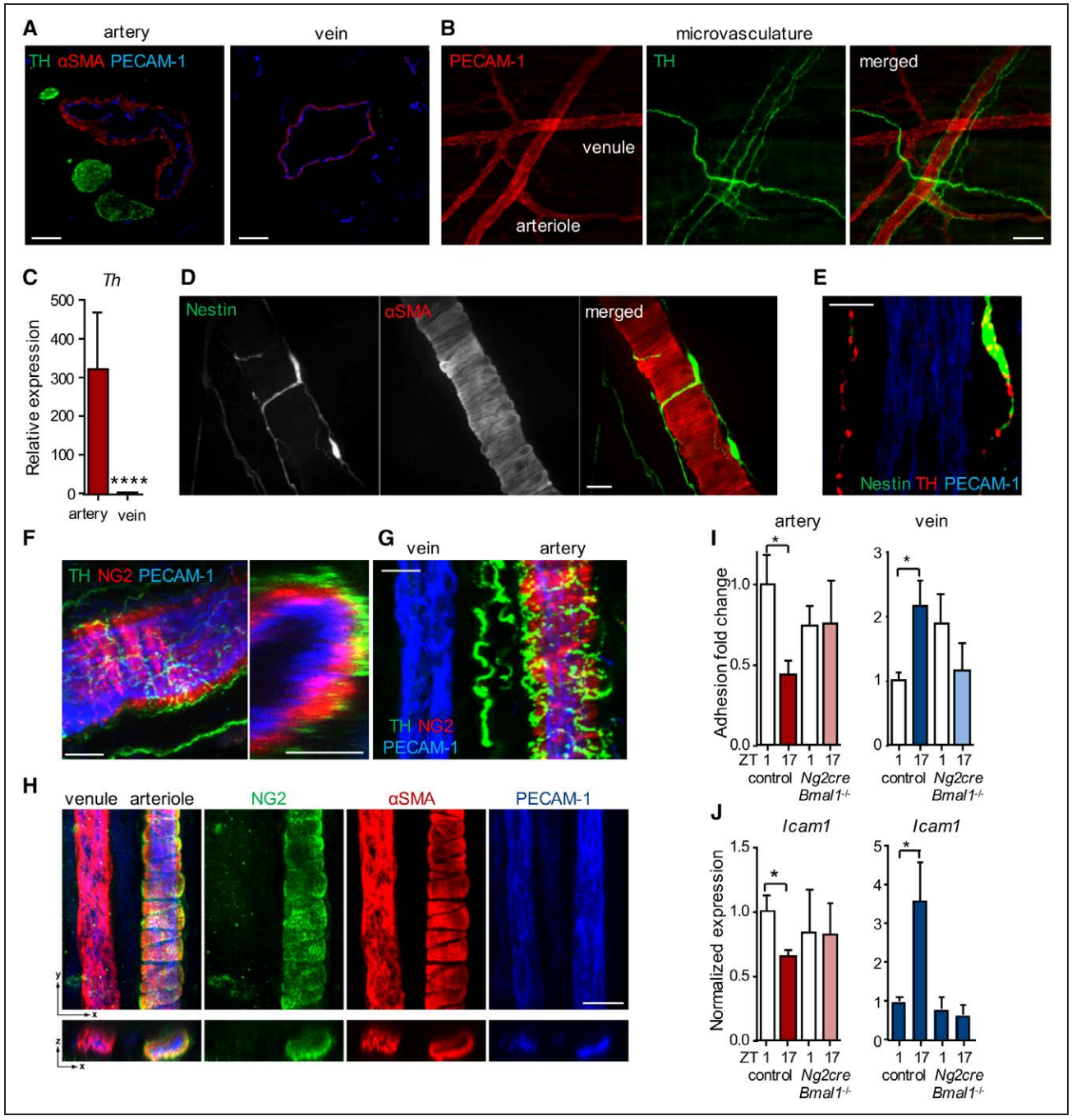

Figure 6. Different sympathetic innervation status of arteries and veins.

A, Immunofluorescence images of carotid artery and jugular vein sections stained with antibodies directed against platelet endothelial cell adhesion molecule-1 (PECAM-1; endothelial cells), α-smooth muscle actin (αSMA; smooth muscle cells), and tyrosine hydroxylase (TH; sympathetic nerves) in steady state. **B**, Whole-mount immunofluorescence images of sympathetic innervation in the cremaster muscle microcirculation in steady state. **C**, Quantitative polymerase chain reaction (qPCR) analyses of *Th* expression levels in steady state; n=11 to 12 mice, Mann–Whitney test. **D**, Whole-mount immunofluorescence images of sympathetic innervation (Nestin) of αSMA$^+$ smooth muscle cells of an arteriole in the cremaster muscle microcirculation in steady state. **E**, TH$^+$ sympathetic varicosities within Nestin$^+$ nerve fibers in close proximity to the arterial vessel wall. **F** and **G**, Whole-mount immunofluorescence images of sympathetic innervation (TH) of mural cells (NG2) within the carotid artery and an associated vein (**G**) in steady state harvested from *Ng2-DsRed* mice. The picture on the **right** in **F** represents an orthogonal view. **H**, Whole-mount immunofluorescence images of a cremasteric arteriole and venule stained with antibodies directed against PECAM-1, NG2, and αSMA in steady state. **I**, In vivo quantification of adherent leukocytes after tumor necrosis factor-α (TNF-α) stimulation in carotid artery (red, **left**) and jugular vein (blue, **right**) of *Ng2cre:Bmal1*$^{-/-}$ mice. Data are normalized to Zeitgeber time (ZT) 1-hour control levels; n=4 to 10 mice, Student *t* test with Welch correction. **J**, qPCR analyses of *Icam1* expression levels after TNF-α stimulation in carotid artery (red, **left**) and jugular vein (blue, **right**) of *Ng2cre:Bmal1*$^{-/-}$ mice. Data are normalized to ZT1 control levels; n=3 to 9 mice, Student *t* test with Welch correction. Scale bars: **A** and **B**, 100 μm; **D**, 10 μm; **E**, 5 μm; **F**, 30 μm; **G**, 15 μm; **H**, 20 μm. **P*<0.05; *****P*<0.0001.

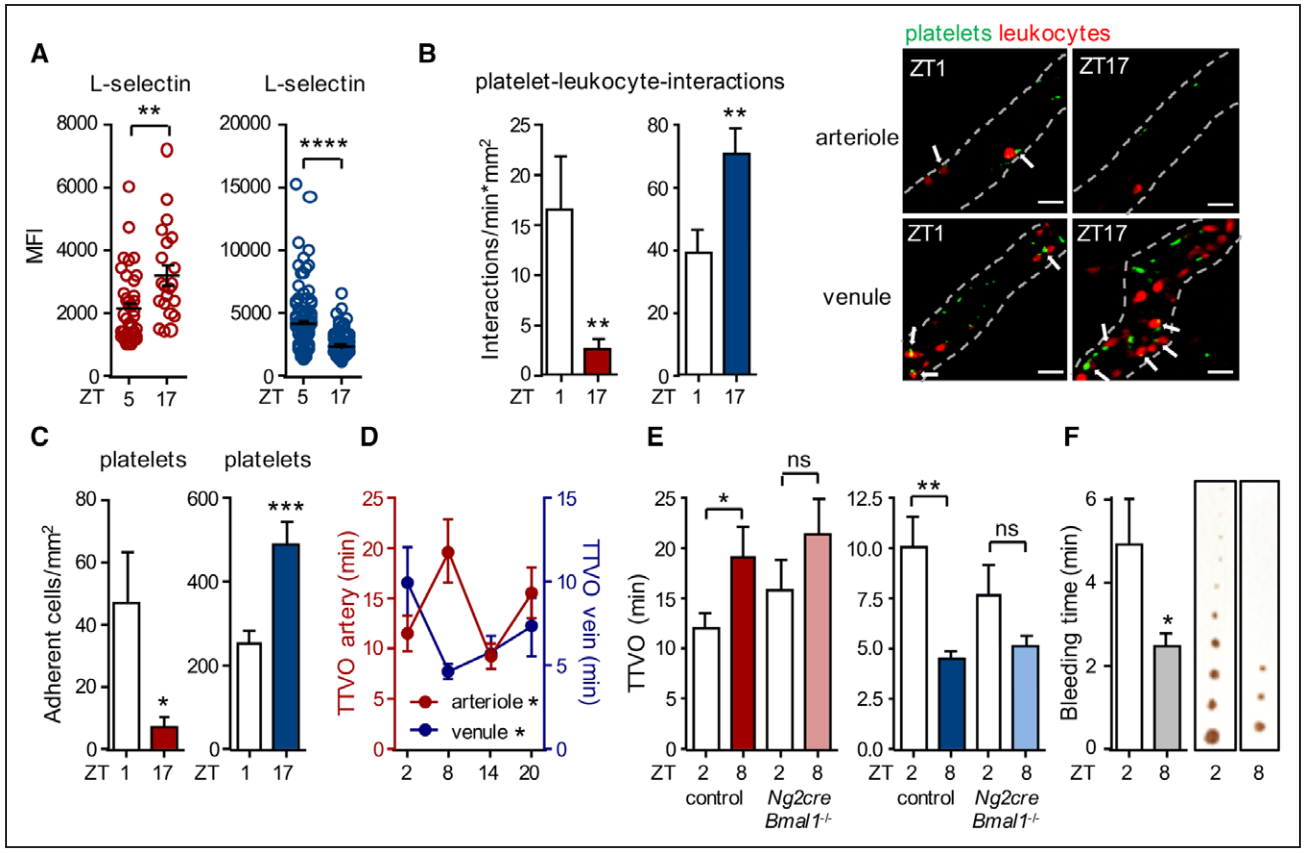

Figure 7. Acute thrombosis in arteries and veins peaks at different times of the day.
A, In vivo quantification of L-selectin mean fluorescence intensity (MFI) levels on the surface of adherent leukocytes after tumor necrosis factor-α (TNF-α) stimulation in cremasteric arterioles (red) and venules (blue); n=24 cells, Student *t* test. **B**, In vivo quantifications of heterocellular interactions between platelets (CD41⁺) and adherent neutrophils (Ly6G⁺) after TNF-α stimulation in cremasteric arterioles (red) and venules (blue); n=28 to 38 vessels, Student *t* test. **C**, In vivo quantification of adherent platelets after TNF-α stimulation in cremasteric arterioles (red) and venules (blue); n=28 to 38 vessels, Student *t* test with Welch correction. **D**, In vivo quantification of time to vaso-occlusion (TTVO) after light-induced thrombus formation in cremasteric arterioles (red) and venules (blue); n=6 to 22 vessels, 1-way ANOVA. **E**, In vivo quantification of TTVO after light-induced thrombus formation in cremasteric arterioles (red) and venules (blue) of control and *Ng2cre:Bmal1*$^{-/-}$ mice; n=12 to 15 vessels, Student *t* test. **F**, Tail bleeding time after 2-mm tail transection, assessed at 2 different time points, with representative images of blood drops on paper every 30 seconds until complete stop of bleeding; n=18 to 20 mice, Student *t* test. ZT indicates Zeitgeber time. Scale bars, 10 μm. **P*<0.05; ***P*<0.01; ****P*<0.001; *****P*<0.0001.

Acute Vaso-Occlusion in Arteries and Veins Peaks at Different Times of the Day

Finally, we explored the relevance of oscillatory leukocyte adhesion patterns in the different vascular beds. We assessed the activation status of adherent leukocytes in situ using L-selectin as a marker because it is shed on aging and activation in the circulation.[35] Interestingly, cells adherent to arteries exhibited lower surface L-selectin levels in the morning, indicating a higher activation status or higher recruitment of aged neutrophils,[35] whereas the inverse was observed in veins (Figure 7A). Thus, not only were more leukocytes recruited at specific times, but also the proportion of activated leukocytes was increased. Adherent L-selectin^{lo} leukocytes were more prone to bind BSA-coated beads that specifically interact with macrophage-1 integrin (Figure VD in the online-only Data Supplement).[3,35] This resulted in more interactions between leukocytes and platelets in arteries in the morning, whereas in veins, more interactions occurred at night (Figure 7B). Analogous to leukocytes, numbers of adherent platelets exhibited a striking diurnal rhythmicity with a phase shift between arteries and veins (Figure 7C). In contrast to leukocytes, systemic platelet counts did not oscillate (data not shown), corroborating the importance of a rhythmic microenvironment for diurnal cellular adhesion. We hypothesized that these interactions might be of relevance for acute thrombotic events. We therefore used a model of phototoxicity-induced thrombus generation, which allowed the well-controlled induction of an acute and local occlusion of arterioles and venules, side by side within the same cremasteric microcirculation. Interestingly, arteries exhibited shorter occlusion intervals at the times of higher cellular adhesion and leukocyte activation in the morning (ZT2 versus ZT8), indicative of a more inflammation-prone environment. In contrast, in veins, shorter occlusion intervals occurred at later times (ZT8 versus ZT2; Figure 7D). These differences were ablated in mice lacking *Bmal1* in NG2⁺

mural cells (Figure 7E), demonstrating that altering circadian oscillations in microenvironmental arterial mural cells had an impact on thrombotic events within the vasculature. We finally assessed whether time-of-day dependency in thrombus formation would still be observable in a general hemostatic model that does not specifically target the venous or arterial vasculature or whether these rhythms would cancel each other out. Performing bleeding assays after tail tip transection, we observed a clear time-of-day difference, with significantly shorter bleeding time occurring at ZT8 compared with ZT2 (Figure 7F). These data thus indicate that timing of venous thrombosis correlates with overall time to bleeding arrest.

DISCUSSION

We show here a striking time-of-day difference in the level of leukocyte adhesion to arteries with an unexpected phase shift from that observed in veins. Our data implicate rhythms in leukocytes as important for the general rhythmicity but point to a critical role of vascular cells in governing vessel type–specific timing in acute vascular inflammation. Although circadian rhythmicity of the clock machinery peaks at similar times in arteries and veins, the timing of an acute inflammatory response is distinct, with promigratory molecules exhibiting their acrophase at different times. We find local sympathetic innervation and β_2-adrenergic receptors to be important in driving vessel type–specific rhythmicity in inflammation in arteries and veins. Although the functional interactions between sympathetic nerves and arteries appear to be direct and involve NG2$^+$ mural cells, the effect on veins appears to be indirect but depends on arterial innervation. Together, our data point to an important role of arteries in driving rhythmic inflammatory responses within the vasculature with effects on the time-of-day–dependent onset of induced acute vaso-occlusive events. Whether these rhythms in TNF-α–driven acute thrombotic events in mice also govern the chronic inflammatory scenarios that culminate in time-of-day cardiovascular events in humans should be the focus of future investigations. Care should be taken, however, when comparing timing in cardiovascular events between humans and mice because, at least with respect to the general ability of blood to clot, these rhythms appear to be inversed between mice and humans.[36,37]

Interplay Between Rhythms of the Vasculature and of Leukocytes

Our data demonstrate that overall rhythmicity in leukocyte adhesion in an inflammatory scenario is dependent on the leukocyte clock. This confirms the role of *Bmal1* in myeloid cells as a critical factor in the generation of rhythmic acute immune responses.[9,21,38] However, myeloid cell rhythmicity does not explain the phase-shifted phenotype between arteries and veins because it affects equally both vessel types. Instead, our homing and expression data implicate the microenvironment in this process. This appears to be at least partly the result of a different level of importance of the endothelial cell clock in both vessels. Whereas in veins endothelial cell–specific *Bmal1* deficiency ablated time-of-day–dependent leukocyte adhesion, in arteries it did not. The reason may be that leukocyte adhesion and emigration from blood generally occur via veins and not arteries. Thus, venous endothelial cells are predestined to recruit leukocytes and to facilitate tissue infiltration compared with arteries, pointing to a more prominent role of the venous endothelial clock in this process. Indeed, although arteries exhibited much more pronounced amplitudes in their circadian gene expression compared with veins, molecules implicated in leukocyte migration, specifically those with an expression in these tissues that is restricted to the endothelium such as E- and P-selectin, showed greater expression amplitudes in veins. Thus, a different contribution of the endothelial cell clock in arteries and veins contributes to the phase shift in inflammatory adhesion rhythmicity.

Robustness of Rhythmicity in Arteries and Veins

The stronger amplitudes in the expression of clock genes in arteries compared with veins point to a more robust circadian rhythm in the former. These data are in line with previous observations demonstrating that arteries exhibit similar acrophases in their circadian amplitudes independently of their respective localization within the body, whereas rhythms in veins can vary significantly by anatomic location.[27] Thus, within the vasculature, robustness in rhythmicity in arteries may be important to preserve blood pressure conformity and stable oxygenation of tissues. Although sympathetic nerves are densely innervating arteries, they appear not to play a role in governing their overall circadian rhythmicity. Instead, local arterial innervation affected rhythms in the inflammatory response. Interestingly, rhythmicity in veins appears to be affected by arteries. This is based on our findings that inflammatory time-of-day effects were lost after local surgical removal of the superior cervical ganglion, which is directly responsible for the sympathetic innervation of local arteries but not veins. In addition, deficiency of *Bmal1* in Ng2$^+$ arterial mural cells ablated daily changes not only in arteries but also in veins. Lastly, pharmacological interference of β-adrenergic signaling resulted in similar effects in arteries and veins; however, arteries were more sensitive to these stimuli.

Thus, venous rhythmicity in the inflammatory response appears to be partly governed by arteries and their associated nerves. Because many of the functions of the sympathetic nervous system are linked to leukocyte trafficking patterns, which classically have been associated with veins, such as the mobilization of leukocytes and *hematopoietic stem cells* from the bone marrow,[39] the recruitment of leukocytes to peripheral tissues,[6] and the retention of lymphocytes within lymph nodes,[40] these may partly be modulated by arteries and their associated sympathetic nerves. How this arterial-venous signal transduction mechanism is achieved and how the potential lag in time may contribute to the phase shift in the inflammatory response are currently unknown and should be the focus of future investigations.

Relevance of Arterial and Venous Leukocyte Recruitment

Although leukocyte trafficking across arterial endothelial cells plays a minor role in the infiltration of cells into tissues and the general amount of leukocytes in tissues, adhesion of cells within the arterial lumen presents a major obstacle for blood flow. Arterial diameters are generally smaller than those of veins because of reduced elasticity compared with veins, which represent the major blood reservoir. Thus, intravascular adhesion within the arterial wall presents a high risk of vascular occlusion with direct effects on blood pressure. Rhythmicity in endothelial cells has previously been linked to the circadian timing of acute thrombotic events.[37] In addition, diurnal rhythms exist with respect to the coagulation cascade and platelet functions.[41] We show that differences in the microenvironment and mural cell clock govern thrombosis in a tissue-specific manner. Taken together, our data point to an intricate interplay between tissue and leukocyte circadian clocks, inflammatory signals, and sympathetic innervation in governing vessel type–specific inflammatory responses.

ARTICLE INFORMATION

Received June 3, 2019; accepted July 8, 2019.

The online-only Data Supplement is available with this article at https://www.ahajournals.org/doi/suppl/10.1161/circulationaha.119.040232.

Authors

Alba de Juan, PhD; Louise Madeleine Ince, PhD; Robert Pick, PhD; Chien-Sin Chen, MS; Filippo Molica, PhD; Gabriele Zuchtriegel, PhD; Chen Wang, MD; Dachuan Zhang, PhD; David Druzd, PhD; Maximilian E.T. Hessenauer, MD; Graziano Pelli, BS; Isa Kolbe, PhD; Henrik Oster, PhD; Colette Prophete, MHSc; Sophia Martina Hergenhan, MS; Urs Albrecht, PhD; Jürgen Ripperger, PhD; Eloi Montanez, PhD; Christoph A. Reichel, MD; Oliver Soehnlein, MD, PhD; Brenda R. Kwak, PhD; Paul S. Frenette, MD; Christoph Scheiermann, PhD

Correspondence

Christoph Scheiermann, PhD, University of Geneva, Centre Médical Universitaire (CMU), Department of Pathology and Immunology (PATIM), Rue Michel-Servet, 1 1206 Geneva, Switzerland. Email christoph.scheiermann@unige.ch or christoph.scheiermann@med.uni-muenchen.de

Affiliations

Walter-Brendel-Centre of Experimental Medicine, University Hospital, Ludwig-Maximilians-University Munich, BioMedical Centre, Planegg-Martinsried, Germany (A.d.J., L.M.I., R.P., C.-S.C., G.Z., D.D., M.E.T.H., S.M.H., E.M., C.A.R., C.S.). University of Geneva, Centre Médical Universitaire (CMU), Department of Pathology and Immunology, Switzerland (L.M.I., F.M., C.W., G.P., B.R. K., C.S.). Ruth L. and David S. Gottesman Institute for Stem Cell and Regenerative Medicine Research and Department of Cell Biology, Albert Einstein College of Medicine, New York (D.Z., C.P., P.S.F.). Institute of Neurobiology, University of Lübeck, Germany (I.K., H.O.). University of Freiburg, Switzerland (U.A., J.R.). Institute for Cardiovascular Prevention (IPEK), Ludwig Maximilian University, Munich, Germany (O.S.). Department of Physiology and Pharmacology (FyFa) and Department of Medicine, Karolinska Institutet, Stockholm, Sweden (O.S.). German Center for Cardiovascular Research (DZHK), Partner Site Munich Heart Alliance, Germany (O.S., C.S.).

Acknowledgments

The authors thank Stéphane Jemelin for technical assistance. The authors are grateful for support from the core facility for animal models of the BioMedical Centre and the animal facility of the Walter-Brendel-Centre of Experimental Medicine.

Sources of Funding

This work was supported by the German Research Foundation (Emmy-Noether grant [SCHE 1645/2-1 to Dr Scheiermann], SFB914 projects B09 and Z03 [Dr Scheiermann] and B08 [Dr Soehnlein], SFB1123 project A6/B5 [Dr Soehnlein], SFB134 and RTG1957 [Dr Oster], and DFG project MO2562/1-2 [Dr Montanez]), the European Research Council starting grant (635872, CIRCODE [Dr Scheiermann]), the Swiss National Foundation (310030_182417/1 [Dr Scheiermann]), the German Centre for Cardiovascular Research and German Ministry of Education and Research, and IMPRS funding (Dr Scheiermann). Dr Oster is funded by a Lichtenberg Professorship of the Volkswagen Foundation. Dr Frenette's laboratory is supported by the National Institutes of Health (DK056638, HL069438, HL116340).

Disclosures

Dr Frenette serves as consultant for Pfizer, has received research funding from Ironwood Pharmaceuticals, and is shareholder of Cygnal Therapeutics. The other authors report no conflicts.

REFERENCES

1. Muller JE, Stone PH, Turi ZG, Rutherford JD, Czeisler CA, Parker C, Poole WK, Passamani E, Roberts R, Robertson T. Circadian variation in the frequency of onset of acute myocardial infarction. *N Engl J Med.* 1985;313:1315–1322. doi: 10.1056/NEJM198511213132103
2. Coller BS. Leukocytosis and ischemic vascular disease morbidity and mortality: is it time to intervene? *Arterioscler Thromb Vasc Biol.* 2005;25:658–670. doi: 10.1161/01.ATV.0000156877.94472.a5
3. Hidalgo A, Chang J, Jang JE, Peired AJ, Chiang EY, Frenette PS. Heterotypic interactions enabled by polarized neutrophil microdomains mediate thromboinflammatory injury. *Nat Med.* 2009;15:384–391. doi: 10.1038/nm.1939
4. Turhan A, Weiss LA, Mohandas N, Coller BS, Frenette PS. Primary role for adherent leukocytes in sickle cell vascular occlusion: a new paradigm. *Proc Natl Acad Sci U S A.* 2002;99:3047–3051. doi: 10.1073/pnas.052522799
5. Xu H, Gonzalo JA, St Pierre Y, Williams IR, Kupper TS, Cotran RS, Springer TA, Gutierrez-Ramos JC. Leukocytosis and resistance to septic shock in intercellular adhesion molecule 1-deficient mice. *J Exp Med.* 1994;180:95–109. doi: 10.1084/jem.180.1.95
6. Scheiermann C, Kunisaki Y, Frenette PS. Circadian control of the immune system. *Nat Rev Immunol.* 2013;13:190–198. doi: 10.1038/nri3386
7. Scheiermann C, Kunisaki Y, Lucas D, Chow A, Jang JE, Zhang D, Hashimoto D, Merad M, Frenette PS. Adrenergic nerves govern circadian leukocyte recruitment to tissues. *Immunity.* 2012;37:290–301. doi: 10.1016/j.immuni.2012.05.021

8. Gibbs J, Ince L, Matthews L, Mei J, Bell T, Yang N, Saer B, Begley N, Poolman T, Pariollaud M, et al. An epithelial circadian clock controls pulmonary inflammation and glucocorticoid action. *Nat Med.* 2014;20:919–926. doi: 10.1038/nm.3599
9. Nguyen KD, Fentress SJ, Qiu Y, Yun K, Cox JS, Chawla A. Circadian gene Bmal1 regulates diurnal oscillations of Ly6C(hi) inflammatory monocytes. *Science.* 2013;341:1483–1488. doi: 10.1126/science.1240636
10. Scheiermann C, Gibbs J, Ince L, Loudon A. Clocking in to immunity. *Nat Rev Immunol.* 2018;18:423–437. doi: 10.1038/s41577-018-0008-4
11. Sumagin R, Sarelius IH. TNF-alpha activation of arterioles and venules alters distribution and levels of ICAM-1 and affects leukocyte-endothelial cell interactions. *Am J Physiol Heart Circ Physiol.* 2006;291:H2116–H2125. doi: 10.1152/ajpheart.00248.2006
12. Ley K, Laudanna C, Cybulsky MI, Nourshargh S. Getting to the site of inflammation: the leukocyte adhesion cascade updated. *Nat Rev Immunol.* 2007;7:678–689. doi: 10.1038/nri2156
13. Muller WA. Transendothelial migration: unifying principles from the endothelial perspective. *Immunol Rev.* 2016;273:61–75. doi: 10.1111/imr.12443
14. Vestweber D. How leukocytes cross the vascular endothelium. *Nat Rev Immunol.* 2015;15:692–704. doi: 10.1038/nri3908
15. Dibner C, Schibler U, Albrecht U. The mammalian circadian timing system: organization and coordination of central and peripheral clocks. *Annu Rev Physiol.* 2010;72:517–549. doi: 10.1146/annurev-physiol-021909-135821
16. Golombek DA, Rosenstein RE. Physiology of circadian entrainment. *Physiol Rev.* 2010;90:1063–1102. doi: 10.1152/physrev.00009.2009
17. Curtis AM, Bellet MM, Sassone-Corsi P, O'Neill LA. Circadian clock proteins and immunity. *Immunity.* 2014;40:178–186. doi: 10.1016/j.immuni.2014.02.002
18. Ishida A, Mutoh T, Ueyama T, Bando H, Masubuchi S, Nakahara D, Tsujimoto G, Okamura H. Light activates the adrenal gland: timing of gene expression and glucocorticoid release. *Cell Metab.* 2005;2:297–307. doi: 10.1016/j.cmet.2005.09.009
19. Ulrich-Lai YM, Arnhold MM, Engeland WC. Adrenal splanchnic innervation contributes to the diurnal rhythm of plasma corticosterone in rats by modulating adrenal sensitivity to ACTH. *Am J Physiol Regul Integr Comp Physiol.* 2006;290:R1128–R1135. doi: 10.1152/ajpregu.00042.2003
20. Vizi ES, Elenkov IJ. Nonsynaptic noradrenaline release in neuro-immune responses. *Acta Biol Hung.* 2002;53:229–244. doi: 10.1556/ABiol.53.2002.1-2.21
21. Gibbs JE, Blaikley J, Beesley S, Matthews L, Simpson KD, Boyce SH, Farrow SN, Else KJ, Singh D, Ray DW, et al. The nuclear receptor REV-ERBα mediates circadian regulation of innate immunity through selective regulation of inflammatory cytokines. *Proc Natl Acad Sci USA.* 2012;109:582–587. doi: 10.1073/pnas.1106750109
22. Zheng B, Albrecht U, Kaasik K, Sage M, Lu W, Vaishnav S, Li Q, Sun ZS, Eichele G, Bradley A, et al. Nonredundant roles of the mPer1 and mPer2 genes in the mammalian circadian clock. *Cell.* 2001;105:683–694. doi: 10.1016/s0092-8674(01)00380-4
23. Chèvre R, González-Granado JM, Megens RT, Sreeramkumar V, Silvestre-Roig C, Molina-Sánchez P, Weber C, Soehnlein O, Hidalgo A, Andrés V. High-resolution imaging of intravascular atherogenic inflammation in live mice. *Circ Res.* 2014;114:770–779. doi: 10.1161/CIRCRESAHA.114.302590
24. Steeber DA, Campbell MA, Basit A, Ley K, Tedder TF. Optimal selectin-mediated rolling of leukocytes during inflammation in vivo requires intercellular adhesion molecule-1 expression. *Proc Natl Acad Sci USA.* 1998;95:7562–7567. doi: 10.1073/pnas.95.13.7562
25. Rot A, von Andrian UH. Chemokines in innate and adaptive host defense: basic chemokinese grammar for immune cells. *Annu Rev Immunol.* 2004;22:891–928. doi: 10.1146/annurev.immunol.22.012703.104543
26. Yoo SH, Yamazaki S, Lowrey PL, Shimomura K, Ko CH, Buhr ED, Siepka SM, Hong HK, Oh WJ, Yoo OJ, et al. PERIOD2::LUCIFERASE real-time reporting of circadian dynamics reveals persistent circadian oscillations in mouse peripheral tissues. *Proc Nat Acad Sci USA.* 2004;101:5339-5346.
27. Davidson AJ, London B, Block GD, Menaker M. Cardiovascular tissues contain independent circadian clocks. *Clin Exp Hypertens.* 2005;27:307–311.
28. Cailotto C, Lei J, van der Vliet J, van Heijningen C, van Eden CG, Kalsbeek A, Pévet P, Buijs RM. Effects of nocturnal light on (clock) gene expression in peripheral organs: a role for the autonomic innervation of the liver. *PLoS One.* 2009;4:e5650. doi: 10.1371/journal.pone.0005650
29. Alito AE, Romeo HE, Baler R, Chuluyan HE, Braun M, Cardinali DP. Autonomic nervous system regulation of murine immune responses as assessed by local surgical sympathetic and parasympathetic denervation. *Acta Physiol Pharmacol Latinoam.* 1987;37:305–319.
30. Reilly DF, Curtis AM, Cheng Y, Westgate EJ, Rudic RD, Paschos G, Morris J, Ouyang M, Thomas SA, FitzGerald GA. Peripheral circadian clock rhythmicity is retained in the absence of adrenergic signaling. *Arterioscler Thromb Vasc Biol.* 2008;28:121–126. doi: 10.1161/ATVBAHA.107.152538
31. Westfall TC, Macarthur H, Byku M, Yang CL, Murray J. Interactions of neuropeptide y, catecholamines, and angiotensin at the vascular neuroeffector junction. *Adv Pharmacol.* 2013;68:115–139. doi: 10.1016/B978-0-12-411512-5.00006-3
32. Kunisaki Y, Bruns I, Scheiermann C, Ahmed J, Pinho S, Zhang D, Mizoguchi T, Wei Q, Lucas D, Ito K, et al. Arteriolar niches maintain haematopoietic stem cell quiescence. *Nature.* 2013;502:637–643. doi: 10.1038/nature12612
33. Murfee WL, Skalak TC, Peirce SM. Differential arterial/venous expression of NG2 proteoglycan in perivascular cells along microvessels: identifying a venule-specific phenotype. *Microcirculation.* 2005;12:151–160. doi: 10.1080/10739680590904955
34. Stark K, Eckart A, Haidari S, Tirniceriu A, Lorenz M, von Brühl ML, Gärtner F, Khandoga AG, Legate KR, Pless R, et al. Capillary and arteriolar pericytes attract innate leukocytes exiting through venules and "instruct" them with pattern-recognition and motility programs. *Nat Immunol.* 2013;14:41–51. doi: 10.1038/ni.2477
35. Zhang D, Chen G, Manwani D, Mortha A, Xu C, Faith JJ, Burk RD, Kunisaki Y, Jang JE, Scheiermann C, et al. Neutrophil ageing is regulated by the microbiome. *Nature.* 2015;525:528–532. doi: 10.1038/nature15367
36. Scheer FA, Shea SA. Human circadian system causes a morning peak in prothrombotic plasminogen activator inhibitor-1 (PAI-1) independent of the sleep/wake cycle. *Blood.* 2014;123:590–593. doi: 10.1182/blood-2013-07-517060
37. Westgate EJ, Cheng Y, Reilly DF, Price TS, Walisser JA, Bradfield CA, FitzGerald GA. Genetic components of the circadian clock regulate thrombogenesis in vivo. *Circulation.* 2008;117:2087–2095. doi: 10.1161/CIRCULATIONAHA.107.739227
38. Curtis AM, Fagundes CT, Yang G, Palsson-McDermott EM, Wochal P, McGettrick AF, Foley NH, Early JO, Chen L, Zhang H, et al. Circadian control of innate immunity in macrophages by miR-155 targeting Bmal1. *Proc Natl Acad Sci USA.* 2015;112:7231–7236. doi: 10.1073/pnas.1501327112
39. Méndez-Ferrer S, Lucas D, Battista M, Frenette PS. Haematopoietic stem cell release is regulated by circadian oscillations. *Nature.* 2008;452:442–447. doi: 10.1038/nature06685
40. Suzuki K, Hayano Y, Nakai A, Furuta F, Noda M. Adrenergic control of the adaptive immune response by diurnal lymphocyte recirculation through lymph nodes. *J Exp Med.* 2016;213:2567–2574. doi: 10.1084/jem.20160723
41. Paschos GK, FitzGerald GA. Circadian clocks and vascular function. *Circ Res.* 2010;106:833–841. doi: 10.1161/CIRCRESAHA.109.211706